

## Links between central CB<sub>1</sub>-receptor availability and peripheral endocannabinoids in patients with first episode psychosis

Alex M. Dickens<sup>1,\*</sup>, Faith Borgan<sup>2,\*</sup>, Heikki Laurikainen<sup>3,\*</sup>, Santosh Lamichhane<sup>1</sup>, Tiago Marques<sup>2</sup>, Tuukka Rönkkö<sup>1</sup>, Mattia Veronese<sup>2</sup>, Tuomas Lindeman<sup>1</sup>, METSY Investigators, Tuulia Hyötyläinen<sup>4</sup>, Oliver Howes<sup>2</sup>, Jarmo Hietala<sup>3</sup>, Matej Orešič<sup>1,5</sup>

<sup>1</sup>Turku Centre for Biotechnology, University of Turku and Åbo Akademi University, Turku, Finland.

<sup>2</sup>Department of Psychosis Studies, Institute of Psychiatry, Psychology & Neuroscience, King's College London, London WC2R 2LS, UK; Psychiatric Imaging Group, MRC London Institute of Medical Sciences, Hammersmith Hospital, Imperial College London, London W12 0HS, UK.

<sup>3</sup>Department of Psychiatry, University of Turku, FI-20520 Turku, Finland; Turku PET Centre, Turku University Hospital, FI-20521 Turku, Finland.

<sup>4</sup>Department of Chemistry, Örebro University, 70281 Örebro, Sweden.

<sup>5</sup>School of Medical Sciences, Örebro University, 70281 Örebro, Sweden.

\*These authors contributed equally to this work.

### Correspondence

Alex M. Dickens, Turku Centre for Biotechnology, University of Turku and Åbo Akademi University, Tykistökatu 6, FI-20520 Turku, Finland.

Email: [alex.dickens@utu.fi](mailto:alex.dickens@utu.fi), Phone: +358 29 450 3798, Fax: +358 29 450 5040

### Keywords

Cannabinoid receptor type 1; endocannabinoid system; first-episode psychosis; positron emission tomography.

## Abstract

There is an established, albeit poorly-understood link between psychosis and metabolic abnormalities such as altered glucose metabolism and dyslipidemia, which often precede the initiation of antipsychotic treatment. It is known that obesity-associated metabolic disorders are promoted by peripheral activation of the endocannabinoid system (ECS). Our recent data suggest that ECS dysregulation may also play a role in psychosis. With the aim of characterizing the involvement of the central and peripheral ECSs and their mutual associations, here we performed a combined neuroimaging and metabolomic study in patients with first-episode psychosis (FEP) and healthy controls (HC). Regional brain cannabinoid receptor type 1 (CB<sub>1</sub>R) availability was quantified in two, independent samples of patients with FEP (n=20 and n=8) and HC (n=20 and n=10), by applying 3D positron emission tomography (PET), using two radiotracers, [<sup>11</sup>C]MePPEP and [<sup>18</sup>F]FMPEP-d<sub>2</sub>. Ten endogenous endocannabinoids or related metabolites were quantified in serum, drawn from these individuals during the same imaging session. Circulating levels of arachidonic acid and oleyl ethanolamide were reduced in FEP individuals, but not in those who were predominantly medication-free. In HC, there was an inverse association between levels of circulating arachidonoyl glycerol, anandamide, oleyl ethanolamide and palmitoyl ethanolamide, and CB<sub>1</sub>R availability in the posterior cingulate cortex. This phenomenon was, however, not observed in FEP patients. Our data thus provide evidence of cross-talk and dysregulation between peripheral endocannabinoids and central CB<sub>1</sub>R availability in FEP.

# Introduction

Psychotic disorders are associated with a reduced life expectancy of 15-20 years<sup>1</sup>, which is in part due to the high prevalence of cardiovascular disease, type 2 diabetes (T2DM) and metabolic syndrome<sup>2, 3</sup>. Unhealthy lifestyles and pharmacological side effects have been suggested to be a major cause of these mortality rates<sup>4</sup>. However, abnormal glucose homeostasis, hyperinsulinemia, dyslipidemia and accumulation of visceral fat are already evident in drug-naïve first episode psychosis (FEP) patients, independent of obesity<sup>5, 6</sup>.

The mechanisms underlying the development of metabolic co-morbidities in psychosis are poorly understood. There is evidence that anti-psychotic medication, particularly clozapine, leads to rapid weight gain<sup>7</sup>, while co-treatment with metformin can help reduce this<sup>8</sup>. A recent study in FEP patients identified changes in specific circulating lipids, which are known to be associated with non-alcoholic fatty liver disease (NAFLD) and T2DM risk, prior to weight gain<sup>9</sup>.

There is emerging evidence suggesting that the endocannabinoid system (ECS) might be dysregulated in various psychiatric disorders, including schizophrenia<sup>10-14</sup>. Furthermore, the ECS has been shown to play a role in metabolic disorders<sup>15-17</sup>. Taken together, these findings suggest that the dysregulation of the ECS could play a role in the development or progression of metabolic co-morbidities observed in psychosis.

The ECS is composed of (1) cannabinoid receptors type 1 (CB1R) and type 2 (CB2R), (2) lipid-derived endocannabinoid ligands with affinity to these or other receptors, and (3) enzymes involved in the synthesis and degradation of these ligands<sup>18, 19</sup>. The CB1Rs are found in the central nervous system (CNS) as well as in the periphery, throughout the gastrointestinal tract, liver, adipose tissue and adrenal glands<sup>20, 21</sup>. In the CNS, the CB1R plays an important role in cognition<sup>22</sup> and has been implicated in mood and anxiety disorders<sup>23, 24</sup>. Recent evidence from both our group and others suggests that central CB1R availability is altered psychosis<sup>25-27</sup>. We recently showed that CB1R

availability is altered in patients with psychosis, where greater reductions in CB<sub>1</sub>R levels are associated with greater symptom severity and poorer cognitive functioning<sup>27</sup>. There is also evidence that endogenous cannabinoid ligands which act as CB<sub>1</sub>R agonists are elevated in the cerebrospinal fluid of medication-naïve psychotic patients<sup>11, 14, 28, 29</sup>.

Metabolomics approaches have identified systemic metabolic changes in the context of psychosis<sup>9, 30, 31</sup> and neurodegenerative disorders<sup>32-34</sup>, suggesting that a strong link exists between the circulating metabolome and diseases of the central nervous system. Several studies have demonstrated that psychotic patients have dysregulated metabolic profiles, including dyslipidemia and dysglycemia<sup>35, 36</sup>. Intriguingly, an imbalance of peripheral endocannabinoids has also been associated with various metabolic disorders, including diabetes and obesity<sup>37, 38</sup>. Furthermore, changes in blood endocannabinoid levels are associated with improvement in symptoms of psychosis<sup>39</sup>, which could imply that endocannabinoid signaling may not only be dysregulated in the central nervous system of psychotic patients, but also in the periphery<sup>12</sup>. There is an association between cannabis use and disturbances of the central ECS, providing further evidence for potential cross-talk between the endogenous peripheral and central ECSs<sup>40, 41</sup>. However, to our knowledge, there are no data investigating the link between peripheral endocannabinoid levels and brain CB<sub>1</sub>R availability in healthy individuals or in psychosis.

Therefore, we aimed to investigate the association between peripheral endocannabinoids and brain CB<sub>1</sub>R availability. To this end, we quantified serum endocannabinoids using liquid-chromatography triple-quadrupole mass spectrometry (LC-QqQMS) and brain CB<sub>1</sub>R availability in a case-control setting, which included FEP patients and matched healthy controls.

## Methods

### Ethics statement

Ethical approvals were obtained from respective study sites in Finland (ETMK 98/180/2013) and

England (14/LO/1289). Subjects' capacities for consent were assessed and informed, written consent was obtained from all volunteers.

## **Study design and participants**

The study setting was described in detail previously<sup>27</sup>. CB1R availability was investigated at two PET centers using independent samples; Turku (n = 11, HC; n = 8, FEP) and London (n = 23, HC; n = 20, FEP). However, some subjects were excluded due to increases in AG levels, caused by sample handling resulting in the following subjects being included in the analysis: Turku (n = 10, HC; n = 8, FEP) and London (n = 15, HC; n = 11, FEP) (**Table 1**). Given putative sex differences in CB1R availability<sup>42</sup>, we only investigated males to remove sex as a source of variability. Corresponding studies in females are currently ongoing.

FEP patients met the following inclusion criteria: (i) DSM-IV diagnosis of a psychotic disorder, determined by the SCID-I/P; (ii) illness duration of less than 3 years; and (iii) male sex. In Turku, FEP volunteers were already taking antipsychotic medication prior to the start of the study and had diagnoses of affective or non-affective psychosis. In London, FEP volunteers were, with the exception of two individuals, medication-free from all pharmacological treatments for at least 6 months and had diagnoses of schizophrenia or schizoaffective disorder (DSM-IV criteria). Healthy volunteers had no current/lifetime history of any Axis-I disorder as determined by the SCID-I/P and were matched for age (age  $\pm$  3 years) and sex (male). Exclusion criteria for all volunteers were: (i) current/lifetime history of substance abuse/dependence; (ii) substance use within the last month; (iii) positive screen on toxicology tests for cannabis and other substances.

## **CB1R availability PET imaging**

The full methods for PET CB1R imaging were described in detail previously<sup>27</sup>. However, a concise description for both studies, Turku and London, is provided here.

**Turku study.** [ $^{18}\text{F}$ ]FMPEP-d2 was synthesized as described previously<sup>43</sup>, with slight modifications. The radiochemical purity was greater than 95% and the molar radioactivity was greater than 500 GBq/ $\mu\text{mol}$  at the end of synthesis resulting in an injected tracer mass below 200 ng.

Positron emission scans were done in three-dimensional list-mode, in increasing frame duration for a total scan range of 0-120 min, with a brain-dedicated high-resolution research tomograph (ECAT HRRT, Siemens Medical Solutions, Kemnath, Germany), after a bolus injection of [ $^{18}\text{F}$ ]FMPEP-d2 ( $201 \pm 11.1$  MBq). Attenuation correction of PET was applied using a  $^{137}\text{Cs}$  point source. Arterial plasma activity was measured continuously for the first 3.5 minutes, and discretely thereafter at 4.5, 7.5, 11, 15, 20, 25, 30, 35, 40, 45, 50 and 60 min. Arterial input was corrected for tracer metabolite activity measured using thin layer chromatography and digital autoradiography. The resulting metabolite free arterial input was corrected for temporal delay between blood and PET tissue measurements. Motion correction between PET frames was done by realigning the PET frames to a single reference frame with the most uptake on average. Whole-brain T<sub>1</sub>-weighted MRI images were acquired by a Philips 3T Ingenuity PET/MR hybrid scanner. The individual T<sub>1</sub>-weighted images were co-registered to the sum of the realigned PET frames. Inverse normalization parameters obtained from normalizing the co-registered T<sub>1</sub>-weighted images to MNI space were used to fit the Hammersmith anatomical atlas to the PET frames (Hammers et. al 2003). Data pre-processing was performed using Statistical Parametric Mapping 12 (<http://www.fil.ion.ucl.ac.uk/spm>) and MATLAB R2014b (Mathworks Inc., Natick, MA).

**London study.** Continuous, 90-minute PET scans were acquired on a PET/CT (Hi-Rez Biograph 6 CT44931; Siemens Medical Solutions, Kemnath, Germany) in three-dimensional mode, after bolus injection of  $314 \pm 34.4$  MBq of [ $^{11}\text{C}$ ]MePPEP, as previously described<sup>44-46</sup>. CT scans were acquired prior to each PET scan for correction of attenuation and scatter. Continuous arterial blood sampling took place for the first 15 minutes of the scan which was followed by discrete blood sampling at 2, 5, 10, 15, 20, 25, 35, 40, 50, 60, 70, 80 and 90 minutes after radioligand injection. Images were

reconstructed with filtered back-projection including corrections for attenuation and scatter. There were no significant group differences in injected mass, injected activity, or specific activity. To aid anatomical localization, each volunteer received a high-resolution structural 3D T<sub>1</sub>-weighted magnetic resonance scan acquired on a General Electric MR750 3T scanner (MR750; GE Healthcare, Chicago, IL).

Data pre-processing was performed using a combination of Statistical Parametric Mapping 12 (<http://www.fil.ion.ucl.ac.uk/spm>) and FSL (<http://www.fsl.fmrib.ox.ac.uk/fsl>) functions, as implemented in MIAKAT (<http://miakat.org>). Motion correction was applied to non-attenuation-corrected images<sup>47</sup>. Non-attenuated corrected frames were realigned to a single “reference” frame (corresponding to that with the highest number of counts) by employing a mutual information algorithm. The transformation parameters were then applied to the corresponding attenuated-corrected dynamic images, creating a movement-corrected dynamic image which was used for subsequent analysis. Realigned frames were then summated to create single-subject motion-corrected maps which were then used for MRI and PET co-registration, prior to PET data quantification. T<sub>1</sub>-weighted structural images were co-registered to the PET image using rigid body transformation. Normalization parameters were obtained by warping the co-registered structural MRI to MNI space (International Consortium for Brain Mapping ICBM/MNI) using bias-corrected segmentation. The inverse of these parameters was used to fit a neuroanatomical atlas to each individual PET scan using the Hammersmith atlas<sup>48</sup>. Whole blood time-activity curves (TACs) were fitted using a multi-exponential function as derived by Feng’s model<sup>49</sup>. For each scan, a time delay was fitted and applied to the input functions (both parent and whole blood TACs) to account for any temporal delay between blood sample measurement and target tissue data. Regions of interest were harmonized with the Turku PET dataset.

In both Turku and London studies, CB<sub>1</sub>R availability was indexed using the volume of distribution (VT ml/cm<sup>3</sup>) of [<sup>11</sup>C]MePPEP, as calculated using the Logan graphical method with a metabolite-

corrected arterial plasma input function. The resulting model was validated as described previously<sup>27,50</sup>. The temporal lobe, frontal lobe, anterior cingulate cortex, posterior cingulate cortex, striatum, parietal lobe, occipital lobe, putamen, nucleus caudatus, insula, amygdala, and whole brain were chosen as regions of interest for PET. Hippocampal, amygdala, superior temporal gyrus, superior frontal, middle frontal, inferior frontal and orbitofrontal subregions were included to explore regional differences within relevant ROI. Due to the use of different PET tracers used in both sites, the CB1R availability data was scaled to unit variance and zero mean within each study, when analyzed together.

### **Analysis of serum endocannabinoids**

The following peripheral endocannabinoids and related structures were measured using a targeted LC-QqQMS method: THC-COOH, arachidonoyl ethanolamide (AEA), N-arachidonoyl dopamine (NADA), 2-arachidonoyl glycerol (2-AG), 1-arachidonoyl glycerol (1-AG), oleyl ethanolamide (OEA), palmitoyl ethanolamide (PEA), 2-arachidonoyl glycerol ether (2-AGE), arachidonic acid (AA) and stearoyl ethanolamide (SEA). The analytical method was developed for serum samples and all solvents were liquid chromatography (LC) grade (Sigma-Aldrich Inc., St. Louis, MO). Initially, the internal standards (10 µL, 100 ng/mL, of THC-COOH-d9, 2-AG-d5, NADA-d8, and AEA-d8 in EtOH) were added to 200 µL of serum in silylated 2 mL glass chromatography vials. The proteins were then precipitated using acetonitrile (400 µL) containing 0.1% v/v formic acid (LC-grade, Sigma-Aldrich). This was done in metal and glass syringes to ensure no contamination from plastic. The samples were then briefly vortexed and placed at -20 °C for 30 minutes. The samples were then centrifuged (10,000 g, 4 °C) for 10 minutes. The supernatant was then removed and placed in fresh silylated vials and stored for no more than 24 hours before solid phase extraction (SPE) of the endocannabinoids.

The solid-phase extraction (SPE, reverse phase HLB, 30 mg sorbent) was performed in 96-well plates (Waters Inc., Milford, MA) and performed on ice to reduce plastic contamination. Initially, 1



mL of ultrapure H<sub>2</sub>O was added to the top of each well. The supernatant was then transferred into H<sub>2</sub>O via a glass Pasteur pipette and gently mixed by pipetting up and down. The vacuum pump (-3 mbar) was then started and the wells allowed to dry. The wells were then washed twice with 15% ACN in ultrapure H<sub>2</sub>O (500 µL, 0.1% v/v formic acid). The pressure was then reduced to -15 mbar and the wells dried for 15 minutes. The waste container under the 96-well sorbet plate was then replaced with 750 µL silylated glass insert vials in a deep 96-well plate. The endocannabinoids were eluted by allowing acetone (350 µL, 0.1% v/v formic acid) to pass through the sorbent bed twice. The samples were then evaporated to dryness under a stream of N<sub>2</sub> prior to resuspension in a 70% solution of ACN (100 µL, 30% ultrapure water, 1% v/v acetic acid). The samples were then vortexed briefly and stored at -20 °C prior to the LC-QqQMS experiment.

The endocannabinoids were separated using ultra-high-performance liquid chromatography (UHPLC). The two eluent solvents were (i) H<sub>2</sub>O (1% v/v acetic acid) and (ii) ACN. The gradient was set up as follows: the initial conditions were 70% B for 4.5 minutes increasing to 80% B by 7 minutes. By 8 minutes, the gradient was increased to 95% B and held there for 10 minutes. The gradient was reduced to the starting conditions by 10.5 minutes and the column flushed with a minimum of 10 column volumes. The flow rate was set at 0.5 mL/min throughout the run and the column temperature set to 60 °C. The column used for the separation was a Waters ACQUITY BEH reverse phase C18 column (130 Å, 1.7 µm, 2.1 mm × 50 mm). The injection volume was 10 µL. The needle was washed three times both before and after the injection with two solvents: (i) IPA:ACN (1:1), and (ii) H<sub>2</sub>O:MeOH (1:1). The mass spectrometer 5500 QTRAP (AB Sciex Inc., Framingham, MA) was set up in scheduled multiple reaction monitoring (MRM) mode which allows for the setup of detection windows around the peak of interest to improve sensitivity. The details of the MRM transitions can be found in **Supplementary Table 1**.

## Statistical Analysis

The non-parametric Mann-Whitney U test was used for comparing the levels of circulating endocannabinoids, and performed using GraphPad Prism v. 7.04 (GraphPad Software Inc., San Diego, CA). In order to compare the association between circulating endocannabinoids with brain CB<sub>1</sub>R availability, two methods were utilized: (i) partial least squares regression (PLS-R) modeling was used in order to combine multiple brain regions and circulating endocannabinoid measures. This analysis was performed using PLS-Toolbox v. 8.6 (Eigenvector Research Inc., Manson, WA) and MATLAB 2017b (Mathworks Inc., Natick, MA). Due to the small number of samples, a leave-one-out cross-validation, using the number of iterations of the smallest group size, was utilized to ensure model validity. (ii) Spearman correlation coefficients were calculated using the statistical toolbox in MATLAB 2017b and p-values < 0.05 (two-tailed) were considered significant for the correlations. The individual spearman correlation coefficients (R) were illustrated as a heatmap using the 'corrplot' package for the R statistical programming language<sup>51</sup>. The individual correlations between the serum endocannabinoids and CB<sub>1</sub>R availability were plotted and analyzed using GraphPad Prism.

### **Generation of the statistical association brain maps**

In order to visualize the associations of CB<sub>1</sub>R availability across different brain regions, the R<sup>2</sup> values from the individual brain regions arising from the PLS-R modelling were mapped onto the same brain template as the PET image analysis using MATLAB 2017b. The resultant image was then visualized using CARIMAS v. 2.9 (Turku PET Centre, Turku, Finland). The color scale for each brain region was defined by the healthy controls in each cohort and then applied to the FEP patients.

## **Results**

### **Levels of circulating endocannabinoids**

We measured a total of ten endocannabinoids and related structures (**Supplementary Table 1**) from serum of both HC and FEP patients from the two study sites. Considerable increases in AG

were observed in some samples, which can be explained by variable freezing times<sup>52</sup>. These samples were excluded from subsequent analyses, resulting in the following available sample numbers: Turku (n = 10, HC; n = 8, FEP) and London (n = 11, HC; n = 15, FEP). In the Turku study, there was a reduction in circulating levels of arachidonic acid (AA;  $140.6 \pm 29.9$  vs.  $104.1 \pm 26.8$  ng/mL) and OEA ( $3.23 \pm 1.04$  vs.  $2.29 \pm 0.50$  ng/mL) in the FEP patients (**Figure 2a**). AA forms the backbone of two major endocannabinoids (AEA and 2-AG)<sup>53</sup>, and is released when they are broken down by fatty acid amide hydrolase (FAAH)<sup>54</sup> and monoacylglycerol lipase (MGL)<sup>55</sup>. Therefore, the decreased levels of AA in FEP suggest reduced breakdown of these two metabolites. In line with this, there is a trend towards an increase in AG observed in the FEP group ( $2.32 \pm 0.94$  vs.  $3.69 \pm 2.02$  ng/mL). Due to the use of serum, it was, however, not possible to differentiate between the levels of 1-AG and 2-AG, because of their rapid isomerization at room temperature. Therefore, only the concentrations of total AG are reported.

The same endocannabinoids were, however, not altered in patients with FEP in the London study (**Figure 2b**). In Turku, patients had already started antipsychotic medication, whilst in London, the patients were mostly drug-naïve or free of pharmacological treatments<sup>27</sup>. Previous literature has shown that endogenous central elevations in anandamide (a CB<sub>1</sub>R agonist) found in patients with FEP<sup>14, 56</sup> are absent in patients taking antipsychotics<sup>56</sup>. Thus, antipsychotic treatment in the Turku sample may account for the differences we observe. However, this discrepancy may also be due to other differences between the study populations, such as diagnosis, substance use, diet or duration of illness.

### **Associations between central and peripheral endocannabinoid systems**

Given the known role of the endocannabinoid system in dietary regulation<sup>57</sup> and weight gain<sup>58</sup>, we next investigated the associations between peripheral endocannabinoid levels and CB<sub>1</sub>R availability.

Initially, we explored how circulating levels of endocannabinoids are associated with CB<sub>1</sub>R availability in the brain in both studies using PLS regression, which allowed us to see how all of the endocannabinoids are associated with individual brain regions in one model. The  $R^2$  values were increased in healthy controls both in the Turku (**Figure 3a**) and London (**Figure 3c**) cohorts, as compared to the FEP group (**Figure 3b**, Turku and **Figure 3d**, London). We next explored the univariate associations between levels of circulating endocannabinoids and CB<sub>1</sub>R availability in the brain. Positive correlations of CB<sub>1</sub>R availability between the brain regions were observed in HCs from both study sites (**Figure 3e**). Similarly, levels of circulating endocannabinoids were also positively correlated with each other in the healthy subjects (**Figure 3e**). Interestingly, the levels of peripheral endocannabinoids and central CB<sub>1</sub>R availability were, conversely, negatively correlated in HCs in both Turku and London samples (**Figure 3e**). In FEP subjects, CB<sub>1</sub>R availability was also positively correlated between the different brain regions (**Figure 3f**). However, the degree of positive correlation between the circulating endocannabinoids was reduced (**Figure 3f**).

Notably, the negative correlations between CB<sub>1</sub>R availability and levels of circulating endocannabinoids, as observed in HC, were absent in FEP patients (**Figures 3e** and **3f**). The loss of this association is more pronounced in the Turku study (**Supplementary Figure 1a-b**) compared to the London study (**Supplementary Figure 1c-d**). This relative lack of association between central CB<sub>1</sub>R availability and circulating endocannabinoid levels in FEP suggests that there may normally be a functional link between these two systems, which may be dysregulated in FEP.

In order to further examine the associations between central CB<sub>1</sub>R availability and circulating peripheral endocannabinoids, we selected the brain region with the highest  $R^2$  value from the PLS-R modeling; the posterior cingulate cortex (**Figure 3**). For the majority of serum endocannabinoids measured in FEP patients, there was a clear loss of any negative correlation with CB<sub>1</sub>R availability, with few positive associations observed in the FEP patients (**Figure 4**). This effect was more

pronounced in the Turku study (**Supplementary Figure 2a**), with similar trends observed in the London study, though these did not reach statistical significance (**Supplementary Figure 2b**).

## Discussion

We demonstrated that the cross-talk between the endocannabinoid networks in the brain and periphery are dysregulated in FEP, as compared to healthy controls. Reduced levels of AA and OEA in FEP subjects were observed in the Turku study, but not in London, where the patients were predominately drug-naïve or free from pharmacological treatments. A negative association between brain CB<sub>1</sub>R availability and serum endocannabinoid levels was observed in healthy individuals, but not in FEP patients across the two independent cohorts of patients.

Endocannabinoids are lipid mediators with a vital role in the maintenance of metabolic and immune homeostasis<sup>59, 60</sup>. Several studies have found that systemic lipid profiles are dysregulated in various psychotic disorders<sup>9, 61</sup>. Our study corroborates these earlier findings, suggesting that the systemic ECS is dysregulated in psychosis<sup>12, 29, 62</sup>. In the periphery, a significant drop in the circulatory endocannabinoid, anandamide, was previously found to accompany the acute phase of schizophrenia<sup>12</sup>. This finding is at odds with findings from the London study as well as previous literature showing that patients with FEP not taking antipsychotics or using cannabis show increased levels of anandamide in cerebrospinal fluid<sup>14, 29, 56</sup>. However, the finding from the Turku study is consistent with previous work showing a downregulation of enzymes involved in the synthesis of endocannabinoid ligands in peripheral blood mononuclear cells (PBMCs) of FEP patients, as compared to matched, healthy controls<sup>62</sup>. In addition to FEP, other neuroinflammatory diseases including multiple sclerosis, Huntington's and Parkinson's diseases, are characterized by ECS alterations in the periphery<sup>63</sup>.

Our previous data links rapid weight gain in FEP with elevated baseline levels of triglycerides of low carbon number and double bond count<sup>9</sup>, which are known to be associated with *de novo*

lipogenesis, inhibition of lipolysis, and NAFLD<sup>64, 65</sup>. Endocannabinoids are known to stimulate *de novo* lipogenesis and obesity<sup>66</sup>. In our previous hepatic venous catheterization study in humans, we found elevated liver fat to be associated both with increased levels of 2-AG as well as higher splanchnic production of triglycerides of low carbon number and double bond count, suggesting that the ECS could contribute to the development of human NAFLD by affecting hepatic lipid metabolism<sup>64</sup>.

OEA is the monounsaturated analogue of AEA, but, unlike AEA, acts independently of the cannabinoid pathway, with no reported direct activity at the two known cannabinoid receptors, CB<sub>1</sub>R and CB<sub>2</sub>R<sup>67</sup>. OEA stimulates fat utilization as a peroxisome proliferator-activated receptor alpha (PPAR $\alpha$ ) agonist<sup>68</sup>. Activation of PPAR $\alpha$  by OEA is known to induce satiety and regulate body weight<sup>69</sup>. A study in mice also suggests that OEA inhibits food intake by recruitment of the brain histaminergic system<sup>70</sup>. Our data suggest that decreased OEA in FEP subjects is likely the effect of antipsychotic medication, as this was not seen in the cohort that was predominately unmedicated. Inhibition of lipolysis due to diminished OEA<sup>69</sup> may also contribute to increased liver fat, *i.e.*, the accumulation of triacylglycerols in the liver, as observed by lipidomics in non-obese FEP patients who subsequently rapidly gained weight<sup>9</sup>. It is thus plausible that OEA levels are an early marker of propensity for FEP patients to gain weight. This hypothesis will clearly need to be examined prospectively, in a larger study setting.

Our study also shows that peripheral endocannabinoids and central CB<sub>1</sub>R availability are inversely correlated in healthy individuals, while no such association is observed in FEP patients. The CB<sub>1</sub>R modulates energy homeostasis *via* both central and peripheral mechanisms<sup>71</sup>. The association between peripheral and central ECS measures suggests common systemic regulation of ECS in healthy individuals, which, however, is absent in FEP. Our findings from the Turku cohort indicate that both central and peripheral measures of the endocannabinoid system were altered in patients with affective / non-affective psychosis who were taking antipsychotic medication. In contrast, our

findings from the London cohort indicate that patients who were predominately medication naïve/free from pharmacological treatments, show central alterations in CB<sub>1</sub>R availability without any alterations in peripheral levels of endocannabinoids. This suggests that peripheral measures of endocannabinoids may not be a useful biomarker for indexing central endocannabinoid dysfunction in schizophrenia, although, alternatively, this negative finding may also be due to the small sample size, or differences in sample clinical characteristics between studies including diagnosis, illness severity and illness duration.

Taken together, our data provides evidence of ECS dysregulation in FEP both centrally<sup>27</sup> and in the periphery, in medicated patients with FEP. Our findings should be considered as preliminary due to our small sample size and partial inconsistency of results. Further studies are clearly needed in order to further examine the cross-talk between the peripheral and central ECSs in health and psychosis.

## **Acknowledgements**

This project has received funding from the European Union's Seventh Framework Programme for project METSY—Neuroimaging platform for characterization of metabolic co-morbidities in psychotic disorders (no. 602478). The authors thank to Aidan McGlinchey for assistance with editing the manuscript.

## **Consortia**

### ***METSY Investigators***

Raimo K R Salokangas, Tuula Ilonen, Päivi Jalo, Akseli Mäkelä, Tiina From, Janina Paju, Anna Toivonen, Reetta-Liina Armio, Mirka Kolkka, Maija Walta, Max Karukivi, Juha Mäkelä, Maria Tikka, Olof Solin, Merja Haaparanta-Solin, Aidan McGlinchey, Juha Pajula, Mark van Gils, Juha M. Kortelainen, Carmen Moreno, Joost Janssen, Javier Santonja, Covadonga M Diaz-Caneja, Miriam

Ayora Rodriguez, Celso Arango, Alberto Rodriguez-Quiroga, Fabian Hernández-Álvarez, Jose L Ayuso-Mateos, Roberto Rodriguez-Jimenez, Angela Ibañez, Jaana Suvisaari, Maija Lindgren, Teemu Mäntylä, Tuula Kieseppä, Outi Mantere, Eva Rikandi, Tuukka T. Raji, Dieter Maier, Elisabeth Frank, Markus Butz-Ostendorf,

## Author contributions

M.O., J.H., and O.H. initiated, designed, and supervised the study. A.D. T.R., T.L., and T.H. acquired serum endocannabinoid data by mass spectrometry. B.F., H.L., T.M., and M.V. acquired neuroimage data. A.D., B.F., H.L., and M.O. analyzed the data. A.D., S.L. and M.O. wrote the first draft of the manuscript. All authors approved the final version.

## References

1. Saha S, Chant D, McGrath J. A systematic review of mortality in schizophrenia: is the differential mortality gap worsening over time? *Arch Gen Psychiatry* 2007; **64**(10): 1123-1131.
2. Ringen PA, Engh JA, Birkenaes AB, Dieset I, Andreassen OA. Increased mortality in schizophrenia due to cardiovascular disease - a non-systematic review of epidemiology, possible causes, and interventions. *Front Psychiatry* 2014; **5**: 137.
3. Mukherjee S, Schnur DB, Reddy R. Family history of type 2 diabetes in schizophrenic patients. *Lancet* 1989; **1**(8636): 495.
4. Arango C, Bobes J, Kirkpatrick B, Garcia-Garcia M, Rejas J. Psychopathology, coronary heart disease and metabolic syndrome in schizophrenia spectrum patients with deficit versus non-deficit schizophrenia: findings from the CLAMORS study. *Eur Neuropsychopharmacol* 2011; **21**(12): 867-875.
5. Pillinger T, Beck K, Gobjila C, Donocik JG, Jauhar S, Howes OD. Impaired Glucose Homeostasis in First-Episode Schizophrenia: A Systematic Review and Meta-analysis. *JAMA Psychiatry* 2017; **74**(3): 261-269.
6. Pillinger T, Beck K, Stubbs B, Howes OD. Cholesterol and triglyceride levels in first-episode psychosis: systematic review and meta-analysis. *Br J Psychiatry* 2017; **211**(6): 339-349.
7. Covell NH, Weissman EM, Essock SM. Weight gain with clozapine compared to first generation antipsychotic medications. *Schizophr Bull* 2004; **30**(2): 229-240.



8. Liu Z, Zheng W, Gao S, Qin Z, Li G, Ning Y. Metformin for treatment of clozapine-induced weight gain in adult patients with schizophrenia: a meta-analysis. *Shanghai Arch Psychiatry* 2015; **27**(6): 331-340.
9. Suvitaival T, Mantere O, Kieseppä T, Mattila I, Pöhö P, Hyötyläinen T *et al.* Serum metabolite profile associates with the development of metabolic co-morbidities in first-episode psychosis. *Transl Psychiatry* 2016; **6**(11): e951.
10. Newell KA, Deng C, Huang XF. Increased cannabinoid receptor density in the posterior cingulate cortex in schizophrenia. *Exp Brain Res* 2006; **172**(4): 556-560.
11. Koethe D, Giuffrida A, Schreiber D, Hellmich M, Schultze-Lutter F, Ruhrmann S *et al.* Anandamide elevation in cerebrospinal fluid in initial prodromal states of psychosis. *Br J Psychiatry* 2009; **194**(4): 371-372.
12. De Marchi N, De Petrocellis L, Orlando P, Daniele F, Fezza F, Di Marzo V. Endocannabinoid signalling in the blood of patients with schizophrenia. *Lipids in health and disease* 2003; **2**: 5.
13. Parolaro D, Realini N, Vigano D, Guidali C, Rubino T. The endocannabinoid system and psychiatric disorders. *Exp Neurol* 2010; **224**(1): 3-14.
14. Leweke FM, Giuffrida A, Koethe D, Schreiber D, Nolden BM, Kranaster L *et al.* Anandamide levels in cerebrospinal fluid of first-episode schizophrenic patients: impact of cannabis use. *Schizophr Res* 2007; **94**(1-3): 29-36.
15. Iannotti FA, Di Marzo V, Petrosino S. Endocannabinoids and endocannabinoid-related mediators: targets, metabolism and role in neurological disorders. *Prog Lipid Res* 2016; **62**: 107-128.
16. Matias I, Di Marzo V. Endocannabinoids and the control of energy balance. *Trends Endocrinol Metab* 2007; **18**(1): 27-37.
17. Di Marzo V, Piscitelli F, Mechoulam R. Cannabinoids and endocannabinoids in metabolic disorders with focus on diabetes. *Handb Exp Pharmacol* 2011; (203): 75-104.
18. Desfossés J, Stip E, Bentaleb LA, Potvin S. Endocannabinoids and Schizophrenia. *Pharmaceuticals* 2010; **3**(10): 3101-3126.
19. Silvestri C, Di Marzo V. The endocannabinoid system in energy homeostasis and the etiopathology of metabolic disorders. *Cell Metab* 2013; **17**(4): 475-490.

20. Pertwee RG. The pharmacology of cannabinoid receptors and their ligands: an overview. *Int J Obes* 2006; **30 Suppl 1**: S13-18.
21. Frank E, Maier D, Pajula J, Suvitaival T, Borgan F, Butz-Ostendorf M *et al*. Platform for systems medicine research and diagnostic applications in psychotic disorders-The METSY project. *Eur Psychiatry* 2018; **50**: 40-46.
22. Borgan F, Beck. K, Butler E, McCutcheon R, Veronese M, Vernon A *et al*. The effects of cannabinoid 1 receptor compounds on memory: a meta-analysis and systematic review across species. . *Psychopharmacology* 2019 (in press): doi: 10.1007/s00213-00019-05283-00213.
23. Hungund BL, Vinod KY, Kassir SA, Basavarajappa BS, Yalamanchili R, Cooper TB *et al*. Upregulation of CB<sub>1</sub> receptors and agonist-stimulated [<sup>35</sup>S]GTPgammaS binding in the prefrontal cortex of depressed suicide victims. *Mol Psychiatry* 2004; **9**(2): 184-190.
24. Neumeister A, Normandin MD, Pietrzak RH, Piomelli D, Zheng MQ, Gujarro-Anton A *et al*. Elevated brain cannabinoid CB<sub>1</sub> receptor availability in post-traumatic stress disorder: a positron emission tomography study. *Mol Psychiatry* 2013; **18**(9): 1034-1040.
25. Hietala J. 42.4 The Endocannabinoid System in First-Episode Psychosis. *Schizophr Bull* 2018; **44**(Suppl 1): S69-S69.
26. Ranganathan M, Cortes-Briones J, Radhakrishnan R, Thurnauer H, Planeta B, Skosnik P *et al*. Reduced Brain Cannabinoid Receptor Availability in Schizophrenia. *Biol Psychiatry* 2016; **79**(12): 997-1005.
27. Borgan F, Laurikainen H, Veronese M, Marques TR, Haaparanta-Solin M, Solin O *et al*. Cannabinoid 1 receptor levels and cognition in 1 patients with first episode psychosis: a positron emission tomography study in two independent cohorts of patients. *JAMA Psychiatry* 2019 (In Press DOI:10.1001/jamapsychiatry.2019.1427).
28. Leweke FM, Giuffrida A, Wurster U, Emrich HM, Piomelli D. Elevated endogenous cannabinoids in schizophrenia. *Neuroreport* 1999; **10**(8): 1665-1669.
29. Minichino A, Senior M, Brondino N, Zhang SH, Godwlewska BR, Burnet PWJ *et al*. Measuring Disturbance of the Endocannabinoid System in Psychosis: A Systematic Review and Meta-analysis. *JAMA Psychiatry* 2019.
30. Kaddurah-Daouk R, McEvoy J, Baillie RA, Lee D, Yao JK, Doraiswamy PM *et al*. Metabolomic mapping of atypical antipsychotic effects in schizophrenia. *Mol Psychiatry* 2007; **12**(10): 934-945.
31. Oresic M, Tang J, Seppanen-Laakso T, Mattila I, Saarni SE, Saarni SI *et al*. Metabolome in schizophrenia and other psychotic disorders: a general population-based study. *Genome Med* 2011; **3**(3): 19.

32. Quinones MP, Kaddurah-Daouk R. Metabolomics tools for identifying biomarkers for neuropsychiatric diseases. *Neurobiol Dis* 2009; **35**(2): 165-176.
33. Oresic M, Hyotylainen T, Herukka SK, Sysi-Aho M, Mattila I, Seppanan-Laakso T *et al*. Metabolome in progression to Alzheimer's disease. *Transl Psychiatry* 2011; **1**: e57.
34. Bogdanov M, Matson WR, Wang L, Matson T, Saunders-Pullman R, Bressman SS *et al*. Metabolomic profiling to develop blood biomarkers for Parkinson's disease. *Brain* 2008; **131**(Pt 2): 389-396.
35. Foley DL, Morley KI. Systematic review of early cardiometabolic outcomes of the first treated episode of psychosis. *Arch Gen Psychiatry* 2011; **68**(6): 609-616.
36. Henderson DC, Vincenzi B, Andrea NV, Ulloa M, Copeland PM. Pathophysiological mechanisms of increased cardiometabolic risk in people with schizophrenia and other severe mental illnesses. *The lancet Psychiatry* 2015; **2**(5): 452-464.
37. Di Marzo V. The endocannabinoid system in obesity and type 2 diabetes. *Diabetologia* 2008; **51**(8): 1356-1367.
38. Jourdan T, Godlewski G, Kunos G. Endocannabinoid regulation of beta-cell functions: implications for glycaemic control and diabetes. *Diabetes Obes Metab* 2016; **18**(6): 549-557.
39. Leweke FM, Piomelli D, Pahlisch F, Muhl D, Gerth CW, Hoyer C *et al*. Cannabidiol enhances anandamide signaling and alleviates psychotic symptoms of schizophrenia. *Transl Psychiatry* 2012; **2**(3): e94-e94.
40. Volk DW, Lewis DA. The Role of Endocannabinoid Signaling in Cortical Inhibitory Neuron Dysfunction in Schizophrenia. *Biol Psychiatry* 2016; **79**(7): 595-603.
41. D'Souza DC, Cortes-Briones JA, Ranganathan M, Thurnauer H, Creatura G, Surti T *et al*. Rapid Changes in CB<sub>1</sub> Receptor Availability in Cannabis Dependent Males after Abstinence from Cannabis. *Biol Psychiatry Cogn Neurosci Neuroimaging* 2016; **1**(1): 60-67.
42. Laurikainen H, Tuominen L, Tikka M, Merisaari H, Armio RL, Sormunen E *et al*. Sex difference in brain CB<sub>1</sub> receptor availability in man. *Neuroimage* 2019; **184**: 834-842.
43. Donohue SR, Krushinski JH, Pike VW, Chernet E, Phebus L, Chesterfield AK *et al*. Synthesis, ex vivo evaluation, and radiolabeling of potent 1,5-diphenylpyrrolidin-2-one cannabinoid subtype-1 receptor ligands as candidates for in vivo imaging. *J Med Chem* 2008; **51**(18): 5833-5842.

44. Bhattacharyya S, Egerton A, Kim E, Rosso L, Riano Barros D, Hammers A *et al.* Acute induction of anxiety in humans by delta-9-tetrahydrocannabinol related to amygdalar cannabinoid-1 (CB<sub>1</sub>) receptors. *Sci Rep* 2017; **7**(1): 15025.
45. Riano Barros DA, McGinnity CJ, Rosso L, Heckemann RA, Howes OD, Brooks DJ *et al.* Test-retest reproducibility of cannabinoid-receptor type 1 availability quantified with the PET ligand [(1)(1)C]MePPEP. *Neuroimage* 2014; **97**: 151-162.
46. Yasuno F, Brown AK, Zoghbi SS, Krushinski JH, Chernet E, Tauscher J *et al.* The PET radioligand [<sup>11</sup>C]MePPEP binds reversibly and with high specific signal to cannabinoid CB<sub>1</sub> receptors in nonhuman primate brain. *Neuropsychopharmacology* 2008; **33**(2): 259-269.
47. Montgomery AJ, Thielemans K, Mehta MA, Turkheimer F, Mustafovic S, Grasby PM. Correction of head movement on PET studies: comparison of methods. *J Nucl Med* 2006; **47**(12): 1936-1944.
48. Hammers A, Allom R, Koepp MJ, Free SL, Myers R, Lemieux L *et al.* Three-dimensional maximum probability atlas of the human brain, with particular reference to the temporal lobe. *Hum Brain Mapp* 2003; **19**(4): 224-247.
49. Tonietto M, Rizzo G, Veronese M, Borgan F, Bloomfield PS, Howes O *et al.* A Unified Framework for Plasma Data Modeling in Dynamic Positron Emission Tomography Studies. *IEEE Trans Biomed Eng* 2019; **66**(5): 1447-1455.
50. Zanotti-Fregonara P, Hirvonen J, Lyoo CH, Zoghbi SS, Rallis-Frutos D, Huestis MA *et al.* Population-based input function modeling for [(18)F]FMPEP-d 2, an inverse agonist radioligand for cannabinoid CB<sub>1</sub> receptors: validation in clinical studies. *PLoS One* 2013; **8**(4): e60231.
51. R Development Core Team. R: A language and environment for statistical computing. R Foundation for Statistical Computing: Vienna, 2018.
52. Fanelli F, Di Lallo VD, Belluomo I, De Iasio R, Baccini M, Casadio E *et al.* Estimation of reference intervals of five endocannabinoids and endocannabinoid related compounds in human plasma by two dimensional-LC/MS/MS. *J Lipid Res* 2012; **53**(3): 481-493.
53. Mechoulam R, Fride E, Di Marzo V. Endocannabinoids. *Eur J Pharmacol* 1998; **359**(1): 1-18.
54. Cravatt BF, Giang DK, Mayfield SP, Boger DL, Lerner RA, Gilula NB. Molecular characterization of an enzyme that degrades neuromodulatory fatty-acid amides. *Nature* 1996; **384**(6604): 83.
55. Dinh TP, Carpenter D, Leslie FM, Freund TF, Katona I, Sensi SL *et al.* Brain monoglyceride lipase participating in endocannabinoid inactivation. *PNAS* 2002; **99**(16): 10819.

56. Giuffrida A, Leveke FM, Gerth CW, Schreiber D, Koethe D, Faulhaber J *et al.* Cerebrospinal anandamide levels are elevated in acute schizophrenia and are inversely correlated with psychotic symptoms. *Neuropsychopharmacology* 2004; **29**(11): 2108-2114.
57. Rask-Andersen M, Olszewski PK, Levine AS, Schiöth HB. Molecular mechanisms underlying anorexia nervosa: focus on human gene association studies and systems controlling food intake. *Brain Res Rev* 2010; **62**(2): 147-164.
58. Engeli S, Böhnke J, Feldpausch M, Gorzelniak K, Janke J, Bátkai S *et al.* Activation of the peripheral endocannabinoid system in human obesity. *Diabetes* 2005; **54**(10): 2838-2843.
59. DiPatrizio NV, Piomelli D. The thrifty lipids: endocannabinoids and the neural control of energy conservation. *Trends Neurosci* 2012; **35**(7): 403-411.
60. Boorman E, Zajkowska Z, Ahmed R, Pariente CM, Zunszain PA. Crosstalk between endocannabinoid and immune systems: a potential dysregulation in depression? *Psychopharmacology (Berl)* 2016; **233**(9): 1591-1604.
61. Narayan S, Head SR, Gilmartin TJ, Dean B, Thomas EA. Evidence for disruption of sphingolipid metabolism in schizophrenia. *J Neurosci Res* 2009; **87**(1): 278-288.
62. Bioque M, García-Bueno B, Macdowell KS, Meseguer A, Saiz PA, Parellada M *et al.* Peripheral endocannabinoid system dysregulation in first-episode psychosis. *Neuropsychopharmacology* 2013; **38**(13): 2568-2577.
63. Centonze D, Battistini L, Maccarrone M. The endocannabinoid system in peripheral lymphocytes as a mirror of neuroinflammatory diseases. *Curr Pharm Des* 2008; **14**(23): 2370-2342.
64. Westerbacka J, Kotronen A, Fielding BA, Wahren J, Hodson L, Perttinen J *et al.* Splanchnic balance of free fatty acids, endocannabinoids, and lipids in subjects with nonalcoholic fatty liver disease. *Gastroenterology* 2010; **139**(6): 1961-1971 e1961.
65. Oresic M, Hyötyläinen T, Kotronen A, Gopalacharyulu P, Nygren H, Arola J *et al.* Prediction of non-alcoholic fatty-liver disease and liver fat content by serum molecular lipids. *Diabetologia* 2013; **56**(10): 2266-2274.
66. Osei-Hyiaman D, DePetrillo M, Pacher P, Liu J, Radaeva S, Bátkai S *et al.* Endocannabinoid activation at hepatic CB<sub>1</sub> receptors stimulates fatty acid synthesis and contributes to diet-induced obesity. *J Clin Invest* 2005; **115**(5): 1298-1305.
67. Woodhams SG, Sagar DR, Burston JJ, Chapman V. The role of the endocannabinoid system in pain. *Handb Exp Pharmacol* 2015; **227**: 119-143.

68. Guzmán M, Verme JL, Fu J, Oveisi F, Blázquez C, Piomelli D. Oleoylethanolamide stimulates lipolysis by activating the nuclear receptor peroxisome proliferator-activated receptor  $\alpha$  (PPAR- $\alpha$ ). *J Biol Chem* 2004; **279**(27): 27849-27854.
69. Fu J, Gaetani S, Oveisi F, Lo Verme J, Serrano A, Rodriguez De Fonseca F *et al.* Oleylethanolamide regulates feeding and body weight through activation of the nuclear receptor PPAR-alpha. *Nature* 2003; **425**(6953): 90-93.
70. Provensi G, Coccurello R, Umehara H, Munari L, Giacobazzo G, Galeotti N *et al.* Satiety factor oleoylethanolamide recruits the brain histaminergic system to inhibit food intake. *Proc Natl Acad Sci U S A* 2014; **111**(31): 11527-11532.
71. Tam J, Hinden L, Drori A, Udi S, Azar S, Baraghithy S. The therapeutic potential of targeting the peripheral endocannabinoid/CB<sub>1</sub> receptor system. *European journal of internal medicine* 2018; **49**: 23-29.

**Table 1.** Demographic characteristics of the study populations. \*p<0.05

	<b>Turku</b>		<b>KCL</b>	
	<b>FEP</b>	<b>HC</b>	<b>FEP</b>	<b>HC</b>
	<b>n = 8</b>	<b>n = 10</b>	<b>n = 15</b>	<b>n = 11</b>
	<b>mean</b>	<b>mean</b>	<b>mean</b>	<b>mean</b>
	<b>(SD)</b>	<b>(SD)</b>	<b>(SD)</b>	<b>(SD)</b>
Age (years)	26.4 (3.6)	27.18 (5.9)	27.1 (5.1)	26.6 (6.9)
BMI (kg/m <sup>2</sup> )	28.2 (6.9)	25.3 (3.7)	25.9 (5.2)	26.3 (4.1)
Years of education	13.3 (1.3)	15.7 (3.2)	n/a	n/a
Illness duration (months)	5.4 (6.8)	n/a	27.1 (10.1)	n/a
BPRS total score sum	65.3 (17.6)*	30.6 (2.4)*	n/a	n/a
BPRS positive score sum	20.0 (7.3)*	9.2 (0.6)*	n/a	n/a
PANSS positive	n/a	n/a	24.4 (5.4)	n/a
PANSS negative	n/a	n/a	42.5 (9.0)	n/a
PANSS general	n/a	n/a	42.53 (9.0)	n/a
PANSS total	n/a	n/a	90.7 (16.6)	n/a

## Figure legends

**Figure 1.** An overview of the experimental design to study associations between brain cannabinoid receptor 1 (CB<sub>1</sub>R) availability and circulating endocannabinoids. **(a)** CB<sub>1</sub>R availability was investigated *in vivo* in male patients with, first episode psychosis (FEP) and healthy controls (HC) using a CB<sub>1</sub>R-selective radiotracer using positron emission tomography (PET) with arterial blood sampling. This study was performed at two study sites using two independent samples in the city of Turku, Finland and an inner-city area of London, United Kingdom. A [<sup>18</sup>F]FMPEP-d<sub>2</sub> PET tracer was used in Turku while [<sup>11</sup>C]MePPEP tracer was used in London. **(b)** Quantification of circulating endocannabinoids was performed in matched FEP and HC subjects using a quantitative liquid-chromatography triple-quadrupole mass spectrometry assay. **(c)** Peripheral differences in endocannabinoids between FEP and HCs were evaluated by univariate statistics. In order to assess if circulatory endocannabinoids associated with CB<sub>1</sub>R availability in the brain, we performed statistical correlation analysis between six endogenous endocannabinoids and seventeen CB<sub>1</sub>R tracer distribution volumes. The correlation analysis was performed separately between FEP and HC for the two study sites.

**Figure 2.** Scatter plots of the levels of circulating endocannabinoids and related structures from both the Turku (top six) and KCL (bottom six) cohorts. \**p* < 0.05.

**Figure 3.** Correlation analysis, performed between peripheral endocannabinoid concentrations and the distribution volumes of brain CB<sub>1</sub>R availability separately for patients with FEP and HC. Correlation brain maps where the *R*<sup>2</sup> values from the PLS regression analysis are projected into the 3D brain regions used for the PET analysis in the healthy controls (**a**, Turku, **c**, London) and FEP patients (**b**, Turku, **d**, London). Spearman correlation coefficients between CB<sub>1</sub>R availability and circulating endocannabinoids in HC from both Turku and London. (**e**, **f**) Spearman correlation coefficients between CB<sub>1</sub>R availability and circulating endocannabinoids in FEP from both Turku and KCL. The CB<sub>1</sub>R availability was combined by first autoscaling the data from each site. The



correlation coefficient values revealed positive correlations between CB<sub>1</sub>R availability in different regions of the brain in both FEP and HC. There was significant negative association between peripheral AEA and PEA concentrations and CB<sub>1</sub>R availability in certain regions of the brain among HCs, and this relationship was absent in FEP patients, at each respective site. Here, the blue gradient represents positive correlation while the red gradient indicates negative correlation (p-values < 0.05).

**Figure 4.** Scatter plots fitted with a linear regression model of CB<sub>1</sub>R availability (combined data from both studies, scaled to zero mean and unit variance within each study separately) in the posterior cingulate cortex (PCC), versus the log-transformed circulating levels of endocannabinoids. The line shows the linear model for each dataset.

**Supplementary Figure 1.** Correlation analysis, performed between peripheral endocannabinoid concentrations and the distribution volumes of brain cannabinoid receptor 1 availability separately between FEP patients HC at the two study sites (a) Spearman correlation coefficients between CB<sub>1</sub>R availability and circulating endocannabinoids in HC from the city of Turku. (b) Spearman correlation coefficients between CB<sub>1</sub>R availability and circulating endocannabinoids in FEP from the city of Turku. The correlation coefficient values revealed positive correlation between CB<sub>1</sub>R availability in different regions of the brain in both FEP and HC. (c) Spearman correlation coefficients between CB<sub>1</sub>R availability and circulating endocannabinoids in HC from an inner-city area of London. (d) Spearman correlation coefficients between CB<sub>1</sub>R availability and circulating endocannabinoids in FEP from inner city area of London. There was significant negative association between peripheral arachidonoyl glycerol (1+2) concentrations and CB<sub>1</sub>R availability in certain regions of the brain among HCs, which was absent in FEP patients, at different sites, respectively. Here, the blue gradient represents positive correlation while the red gradient indicates negative correlation (p-values < 0.05).

**Supplementary Figure 2.** (a) Scatter plots fitted with a linear regression model of CB1R availability in the posterior cingulate cortex (PCC) versus the log-transformed circulating levels of endocannabinoids from the Turku cohort. (b) Scatter plots fitted with a linear regression model of CB1R availability in the posterior cingulate cortex (PCC) versus the log-transformed circulating levels of endocannabinoids from the London cohort. The line shows the linear model for each dataset.

**Figure 1**

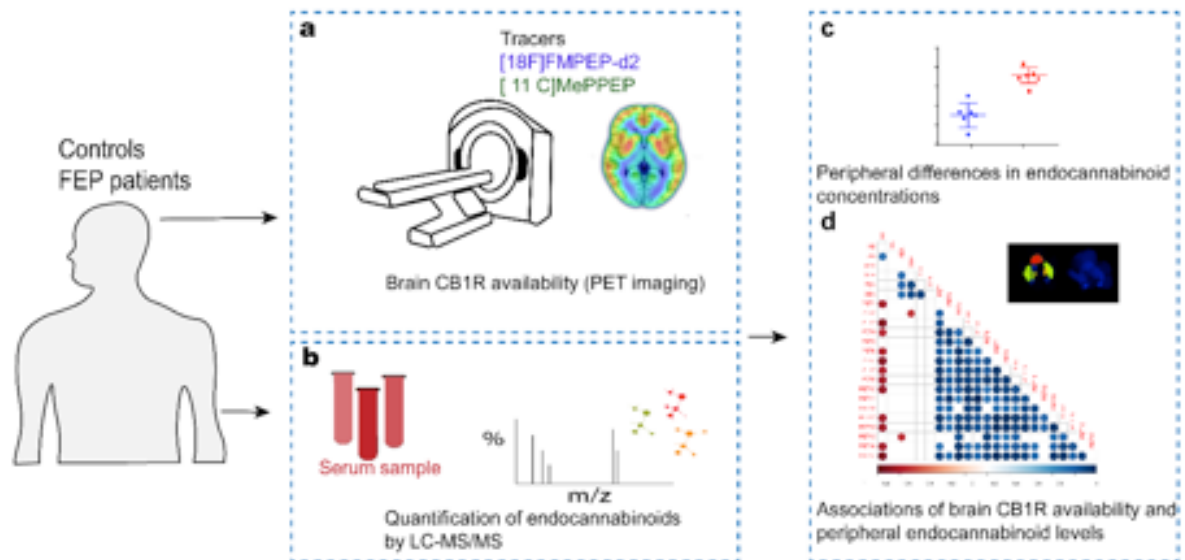


Figure 2

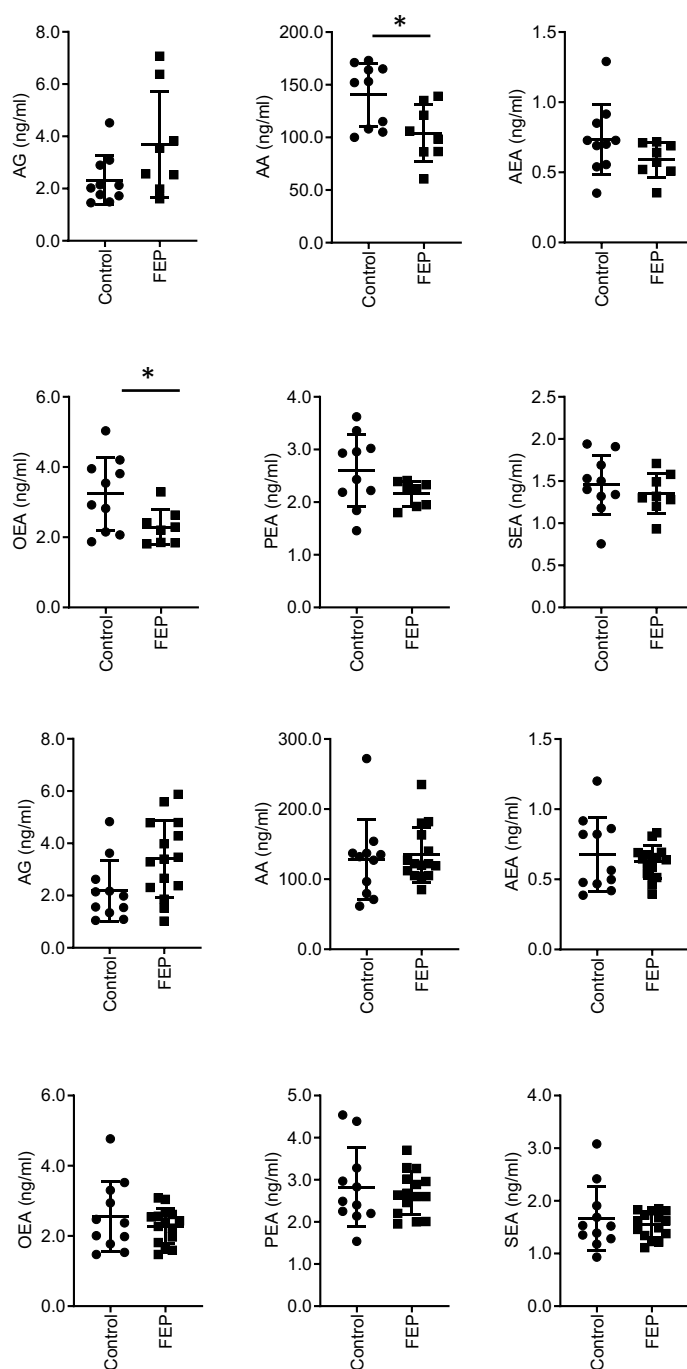


Figure 3

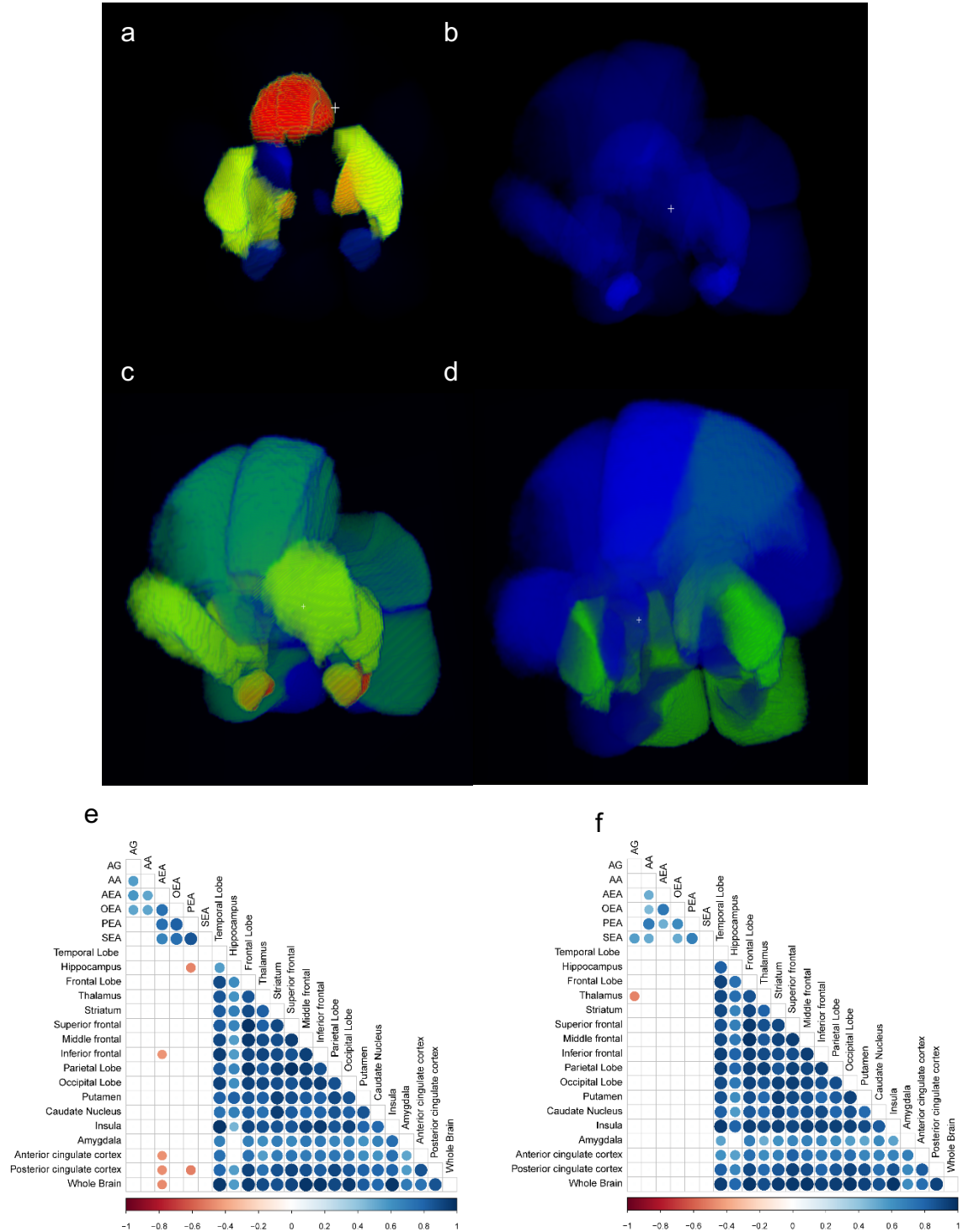
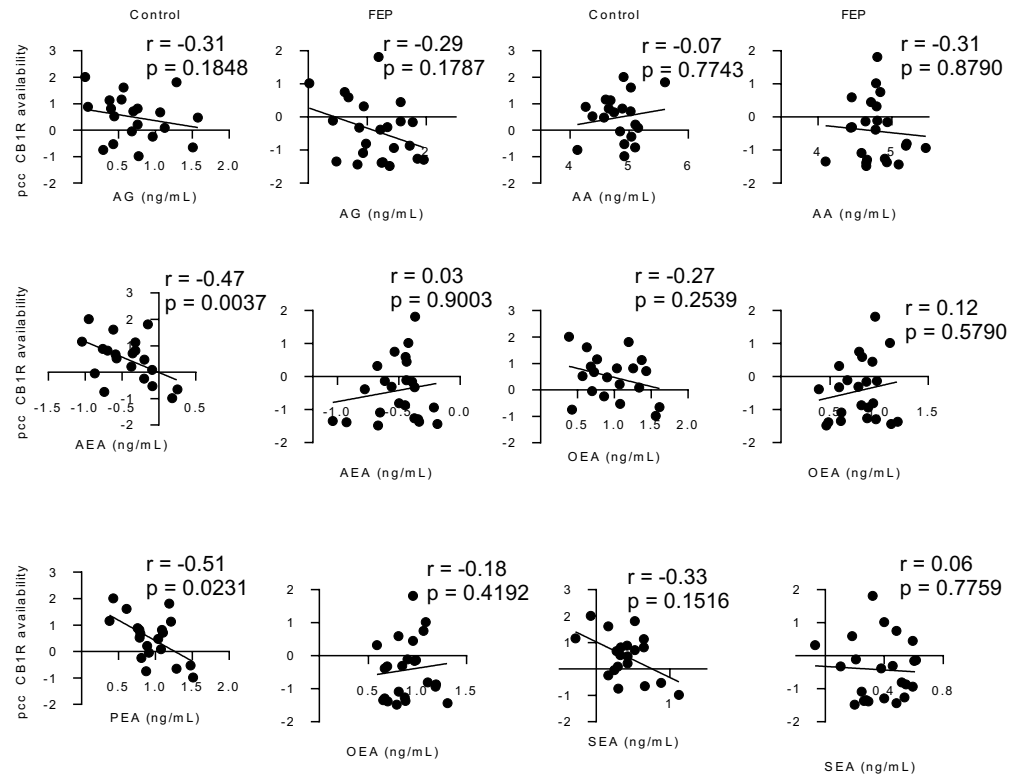


Figure 4

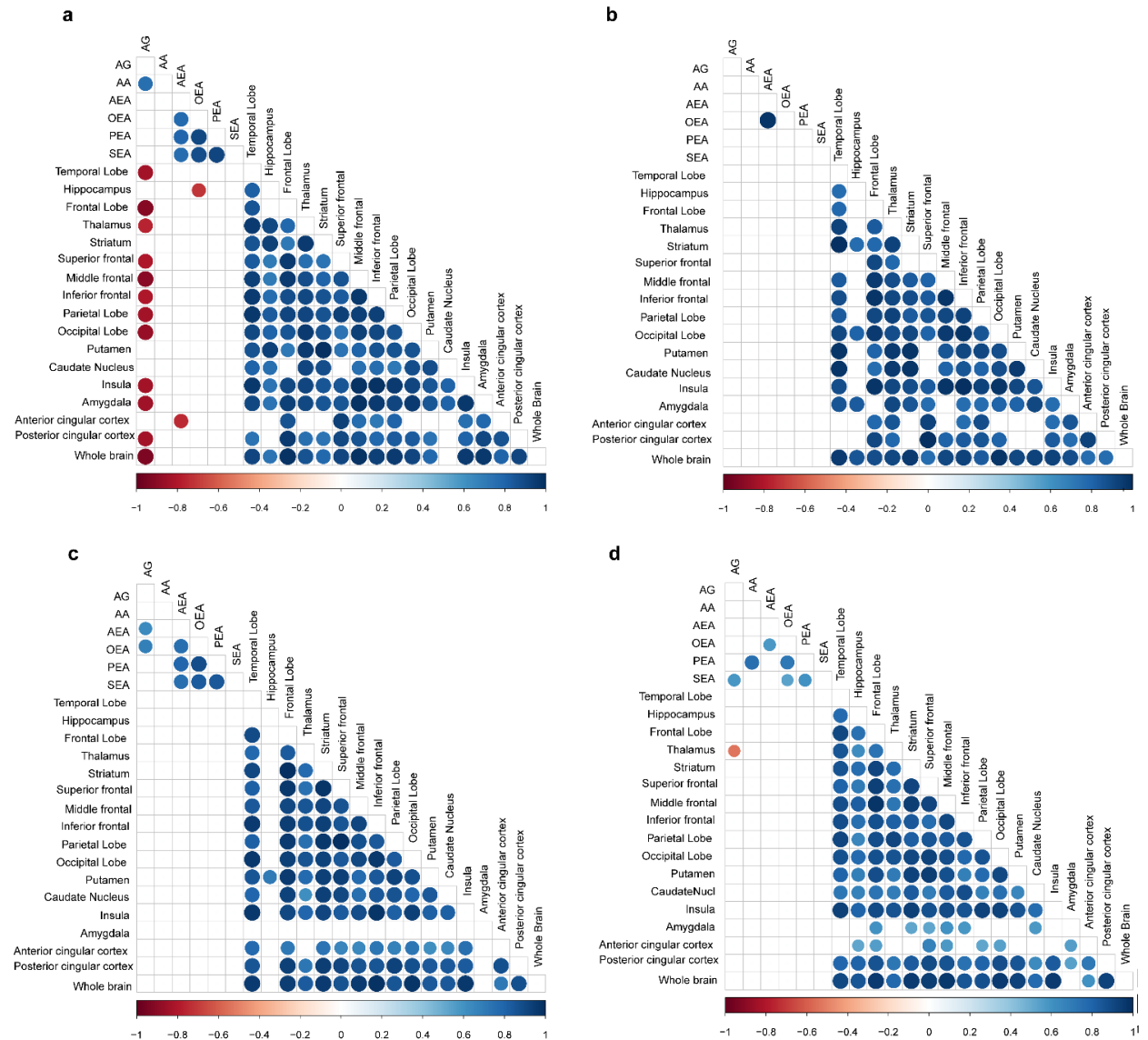


**Supplementary Table 1.** Tandem MS analysis of endocannabinoids. Information on quantification and selective reaction monitoring (SRM) transitions for identification.

Compound	Ionization	Ion Type	Retention		SRM (amu)	CE (eV)
			Time	Internal Standard		
THC-COOH	Negative	Quantifier	1.23	THC-COOH d9	343.400 → 245.100	-32
THC-COOH	Negative	Qualifier	1.23	THC-COOH d9	343.400 → 299.000	-32
PEA	Positive	Quantifier	3.13	AEA-d8	300.400 → 62.100	19
PEA	Positive	Qualifier	3.13	AEA-d8	300.400 → 283.100	19
1-AG	Positive	Quantifier	3.24	2-AG d5	379.300 → 287.300	21
1-AG	Positive	Qualifier	3.24	2-AG d5	379.300 → 203.200	21
2-AG	Positive	Quantifier	2.97	2-AG d5	379.300 → 287.300	21
2-AG	Positive	Qualifier	2.97	2-AG d5	379.300 → 203.200	21
2-AGe*	Positive	Quantifier	3.23	2-AG d5	365.400 → 273.200	20
2-AGe*	Positive	Qualifier	3.23	2-AG d5	365.400 → 121.000	20
NADA*	Positive	Quantifier	2.69	NADA d8	440.300 → 137.100	30
NADA*	Positive	Qualifier	2.69	NADA d8	440.300 → 154.100	30
AEA	Positive	Quantifier	2.26	AEA-d8	348.300 → 62.100	32
AEA	Positive	Qualifier	2.26	AEA-d8	348.300 → 133.100	32
OEA	Positive	Quantifier	3.61	AEA-d8	326.300 → 62.100	20
OEA	Positive	Qualifier	3.61	AEA-d8	326.300 → 309.300	20
AA	Negative	Quantifier	4.48	AA-d8	303.300 → 259.100	-20
AA	Negative	Qualifier	4.48	AA-d8	303.300 → 58.900	-20
SEA	Positive	Quantifier	5.92	AEA-d8	328.400 → 62.100	23
SEA	Positive	Qualifier	5.92	AEA-d8	328.400 → 311.400	23

\*Analyte below limit of detection in study samples.

## Supplementary Figure S1





## Supplementary Figure S2

